Osseointegration Assessment Of Nano Laser-Engraved Implant Surface Treatment Versus Porous Implant Prepared By Laser Sintering Of Titanium Powder

Amr Elkarargy [1], Mostafa Omran [2], Alaa abdelhamid [1], Mahmoud Sallom [3]

[1.] Department of Periodontics, Faculty of Dentistry, Qassim University, KSA
[2.] Department of Prosthodontics, Faculty of Dentistry, Qassim University, KSA
[3.] Department of Prosthodontics, Faculty of Dentistry, Faros University, ARE
dr.amr.elkarargy@qudent.org

Abstract: The main objective for developing implant surface modifications is to promote osseointegration, with faster and intimate contact bone formation. The purpose of this study is to assess histologically and histomorphometrically the role of surface characteristics and manufacturing technique of two unique dental implant systems. The first one relies on engraving the titanium surface using laser to produce nano-sized grooves, while the second depends on selective laser-sintering technique as an additive prototyping method. Twelve New Zealand white mature male rabbits weighting 2.5- 4 kg were selected. Each rabbit received two implants, one in each tibia. Tapered internal Biohorizons implant (TIB) was placed in the right limb; whilst on the contralateral side Internal hex Tixos (IHT) was selected. Six rabbits were sacrificed after 4 weeks then the others after 8 weeks for histological and histomorphometrical assessment. The mean area percent filled by bone trabeculae 4 weeks post-operatively was greater in the TIB group (62.31± 13.38) compared to the IHT group (59.38±12.15) with no statistically significant difference (p=0.7263). On the contrary, eight weeks post-operatively, the area percent of bone trabeculae was greater in the IHT group (90.66±2.87) compared to the TIB group (83.3±3.92). With statistically high significant difference (p=0.0095). Advances in the laser technology as a manufacturing tool leads to highly improved implant surface treatment and so enhanced oseointegration. According to the current study, the implant surface roughness created by selective laser sintering provided better environment for osseointegration than that produced by engraving microgrooves on titanium surface by nano-laser ablasion.
[Amr Elkarargy, Mostafa Omran, Alaa abdulhamid, Mahmoud Sallom. **Osseointegration Assessment Of Nano Laser-Engraved Implant Surface Treatment Versus Porous Implant Prepared By Laser Sintering Of Titanium Powder.** *Life Sci J* 2013;10(4):2201-2211] (ISSN:1097-8135). http://www.lifesciencesite.com. 294

Keywords: Dental implant, Osseointegration, Selective laser-sintering, Laser-lok.

1. Introduction

The biocompatibility of implant material in the human body is related to the interaction between living cells and material of the implant surface (Huang et al., 2005 and Faria et al., 2003).

Titanium and its alloys are widely used for orthopedic and implant dentistry because of their low-density, good mechanical properties (elastic modulus, toughness and fatigue strength) and biochemical inertness (Ellingsen, 1998).

However, the difference in stiffness value between titanium and bones is undesirable and may lead to damaging resorption through stress-shielding phenomenon (Turner et al., 1986).Stiffness of a metal is determined by its Young's modulus as well as its area of moment inertia, that is far higher than that of cortical bone in case of dental implants (Reilly et al., 1974 and Rho et al., 1999).

Beside implant shape (macro-scale), surface properties on micro and nanometric scale could affect the formation of adjacent bones. These surface properties (composition, energy and topography) are interrelated and very difficult to decide how coatings or surface modifications, or both, affect osseointegration. Thus, manufacturers have continuously developed new implants macro-design and surface treatment using clinical trials and investigations (Barewal et al., 2003 and Cooper, 2000). Most surface modifications of clinically available oral implants employ techniques that increase surface roughness, compared with the machined titanium surface. This roughness results to surface irregularities with different forms, shapes and sizes. Thus, most of these roughened surfaces are produced either by coating, blasting or abrading methods using different material particles and/or by chemical methods (Esposito et al., 2005, Esposito et al., 2002, Esposito et al., 2007 and Esposito et al., 2003).

The microtopographic profile of dental implants is defined for surface roughness as being in the range of 1–10μm. This range of roughness maximizes the interlocking between mineralized bone and the surface of the implant (Biela et al., 2009 and Geblinger et al., 2010). In addition, a theoretical approach suggested that the ideal surface should be

covered with hemispherical pits approximately 1.5µm in depth and 4µm in diameter (Martinez et al., 2009). Surface profiles in the nanometer range play an important role in adsorbing proteins, adherence of osteoblastic cells and thus enhancing osseointegration. Subsequently, this nano-surface is essential for osteoblastic cell adhesion and rapid bone apposition. On the other hand, the optimal surface nano-topography for selective adsorption of proteins is unknown and difficult to generate reproducible surface roughness in the nanometer range with some surface treatments as chemical treatment (Asaoka et al., 1985, Yue et al., 1984 and Okazaki et al., 1991).

Recently, the development of direct laser metal sintering (DLMS) has substantially broadened the application of titanium alloys in the dental field and so allowed implants to be produced more economically than by traditional techniques. Among the several direct metal forming techniques, selective laser-sintering (SLS) offers great potential benefits in the field of the biomaterials. SLS has the capability to directly build three-dimensional (3D) metallic components from metal powder with minimal or no post-processing requirements (Lifland and Okazaki, 1993 and Yang et al., 2008).

Deckard and Beaman (1988) were pioneer by using the selective layer laser sintering process. They directly fuses a localized region of a thin layer of metal powder by applying a high-energy focused laser beam in accordance with a sliced 3D computer aided design (CAD) model. Accordingly, through rapid prototyping technique, it is possible to create dental implants from three-dimensional CAD model.

The purpose of this study is to assess histologically and Histomorphometrically the role of surface characteristics and manufacturing technique of two unique dental implant systems. The first system relies on engraving the titanium surface using laser to produce nano-sized grooves while the second system depends on selective laser-sintering technique as an additive prototyping method.

2. Material and Methods

a- Experimental model

This experiment was conducted on a total of twelve New Zealand white mature male rabbits weighting 2.5- 4 kg. The animals were housed in separate cages in temperature - controlled rooms and were fed on standard food and had free access to tap water. The animals were cared for according to the guidelines of the local Ethics Committee of the Animal Research at the Faculty of Medicine, Cairo University, which approved the project before the beginning of the experiments.

Each rabbit received two implants, one in each tibia; the implant in the right limb was Tapered internal Biohorizons (TIB) (Tapered Internal dental implant system, Biohorizons Co., USA), whilst on the contralateral side was Internal hex Tixos (IHT) (Internal hex, Leader Italia Srl., Italy).

b- Surgical procedure

Rabbits were anaesthetized intramuscularly with a mixture of Xylazine (Chanazine, Chanelle Pharmacuetical, Ireland) 5mg/kg body weight and ketamine hydrochloride (Ketamine, Pharmazeutische Pröparate, Germany) 30 mg/kg body weight.

Once general anesthesia was established, the medial aspects round the proximal tibia were shaved and the skin was carefully swabbed with mixture of iodine and 70% ethanol. A 30 mm incision was made along the medial aspect of the proximal tibia and the wound advanced down to and through the periosteum. A subperiosteal dissection was then advanced up to the inferior attachment of the knee joint capsule and laterally to the full extent of the flat medial bone surface.

Under continuous irrigation with sterile saline, the implants installation procedure in tibiae bone was carried out according to the manufacturer's instructions. The prophylactic administration of procaine penicillin (Wyeth Pharmaceuticals, Parramatta, New South Wales.) 60 000 units/kg intramuscularly was commenced during the surgery and continued for three postoperative days to reduce the potential for wound infection.

c- Animal sacrifice

Six rabbits were sacrificed after 4 weeks then the others after 8 weeks for histological and histomorphometrical studies using an intramuscular injection of 60 mg/ml/kg body weight sodium phenobarbitone (Phenobarbitone, Fawns & McAllan Pty Ltd, Melbourne, Victoria).

d- Histological Examination

The tibia were dissected and fixed in 10 percent normal saline for 48 hours. After that time, the specimens were decalcified with a 50 percent formic acid and 20 percent sodium citrate solution for 6 weeks. After eighteen days of decalcification, the implant was removed from the bony tissue by an incision following the implant long axis. Following fixation and decalcification, the bone was embedded in paraffin; serial 6-µm sections were obtained and stained with Hematoxylin and eosin (H & E) and Masson's trichrome.

e- Measuring of the area percent of bone trabeculae

The area percent of bone trabeculae was estimated using Leica Quin 500 analyzer computer system, (Leica Microsystems, Swizerland). The cursor was used to outline the areas of bone trabeculae, which were then masked by a blue binary color that could be measured by the computer. The image analyzer is calibrated automatically to convert

the measurement units (pixels) produced by the image analyzer program into actual micrometer units. The area percent of bone trabeculae was estimated in 5 different fields in each slide using magnification (x100), (Fig.1). Mean values and standard deviation were calculated for each group.

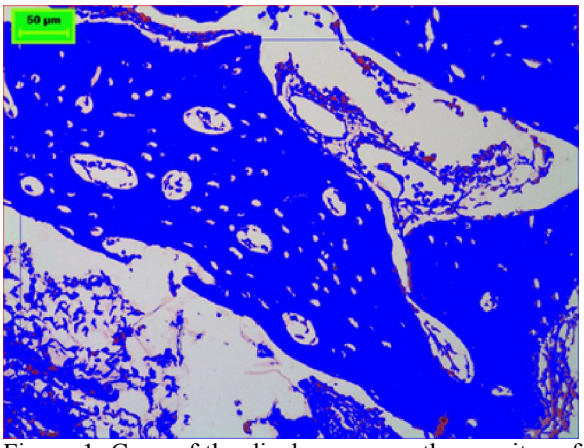

Figure 1. Copy of the display seen on the monitor of the image analyzer revealing areas of bone trabeculae in IHT group (8 weeks post-operatively) covered by a blue binary color that could be measured by the computer system.

Statistical analysis:

The data obtained from computer image analysis were presented as mean and standard deviation (SD), tabulated and statistically analyzed. Student's t test was used for statistical analysis of the difference between groups. P value $\geq$ 0.05 was considered statistically significant

3. Results

I-Four weeks post-operatively

In the Tapered internal Biohorizons (TIB) group, four weeks post-operatively, loose connective tissue, including capillary angiogenesis, was predominant around the implants' sites. Newly formed bone appearing in the form of irregular trabecule of circular or oval shapes could also be observed at the interface between the implant site and the original bone. Indentations demarcating the irregularities in the surface of the implant were still noted in the original bone. Viability of both the newly formed and the original bone was demonstrated by the presence of osteocytes entrapped in lacunae inside the bone trabecule, in addition to osteoblasts bordering their surface (Fig 2, 3, 4&5).

In Internal hex Tixos (IHT) group, 4 weeks post-operatively, dense mature collagen fibers characterized by their parallelism were observed around the implant site. These fibers were supplied by tiny dispersed blood capillaries. Irregular newly-formed bone trabeculae enclosing viable osteocytes were bordering the implant site. Vascular marrow was noted within the newly formed trabeculae and at the interface between the newly-formed and the original bone (Fig 6, 7, 8&9).

ii- Eight weeks post-operatively

In the Tapered internal Biohorizons (TIB) group, eight weeks post-operatively, irregular newly formed bone trabeculae attempted to fill the gap between the implant and the original bone. The viability of these trabeculae was confirmed by the presence of entrapped osteocytes within this osteoid tissue. Moreover, osteoblastic rimming indicated their continuous deposition. Reversal lines denoting the rhythmic pattern of deposition of the newly formed osteoid tissue were also demonstrated. Dilated blood vessels and extravasated red blood cells were seen inbetween the newly formed bone. Regular collagen deposition of variable densities was also detected (Fig.10, 11, 12 &13).

In Internal hex Tixos (IHT) group, 8 weeks post-operatively, numerous regular parallel newly formed bone trabeculae bordered the implant site. Entrapped osteocytes were noted inside these trabeculae, while osteoblasts rimmed their border. The newly formed osteoid trabeculae were separated by parallel collagen fibers supplied by blood capillaries. Dilated blood vessels filled the marrow spaces between the newly-formed and the original bone (Fig.14, 15, 16 &17).

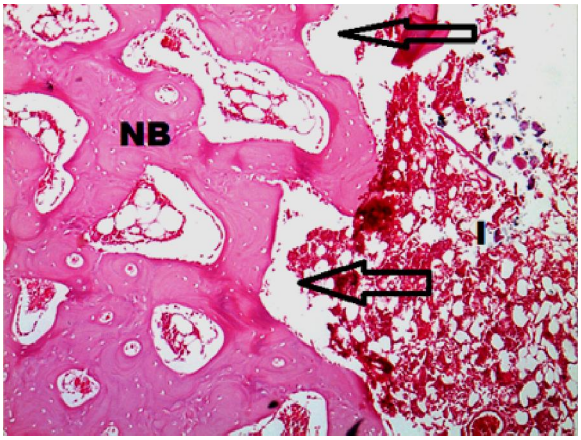

Figure 2. Photomicrograph of TIB group, 4 weeks post-operatively revealing the formation of connective tissue and predominant capillary angiogenesis around the implant site (I). The indentations (arrows) related to the surface of the implant are noted in the original bone (NB) that bordered the implantation site (H&E x100).

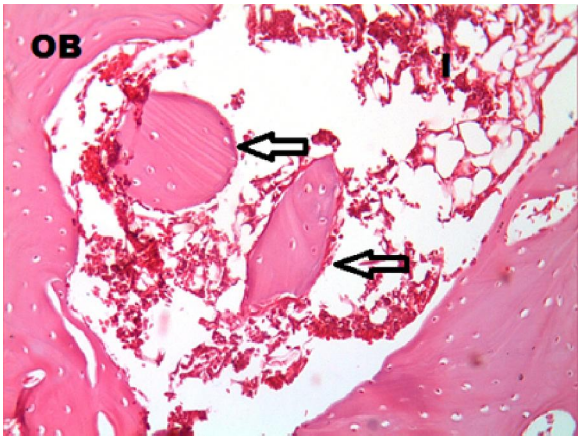

Figure 3. Photomicrograph of TIB group, 4 weeks post-operatively revealing the presence of vascular connective tissue around the implant site (I). Irregular oval and rounded bone trabeculae (arrows) are formed in the interface between the implantation site and the original bone (OB) (H&E x200).

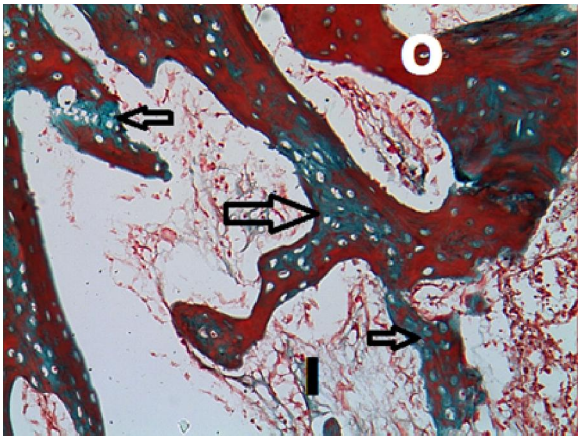

Figure 5. Photomicrograph of (TIB) group at 4 weeks revealing thin trabeculae of newly formed bone (arrows) stained blue- green with Masson's trichrome bordering the implant site (I). Original bone (O) stained red is seen at the periphery (Masson's trichrome x200).

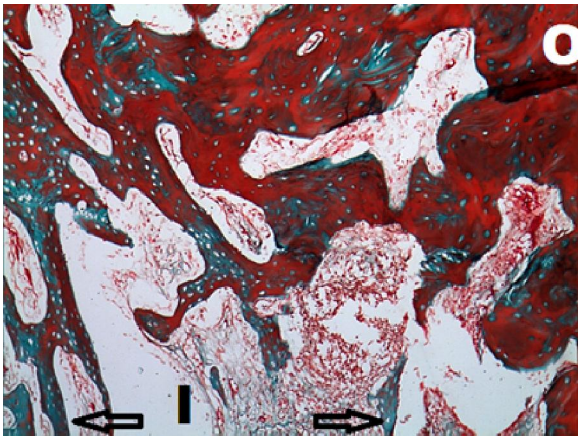

Figure 4. Photomicrograph of (TIB) group at 4 weeks revealing thin trabeculae of newly formed bone (arrows) stained blue- green with Masson's trichrome bordering the implant site (I). Original bone (O) stained red is seen at the periphery (Masson's trichrome x100).

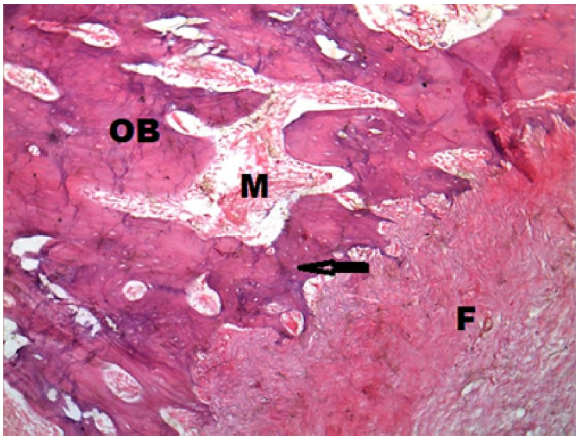

Figure 6. Photomicrograph of (IHT) group, 4 weeks post-operatively revealing the presence of dense fibrous connective tissue (F) around the implant site. Irregular newly-formed bone trabeculae enclosing viable osteocytes (arrows) were bordering the fibrous tissue. Vascular marrow (M) separated the newly-formed osteoid tissue from the original bone (OB), (H&E x100).

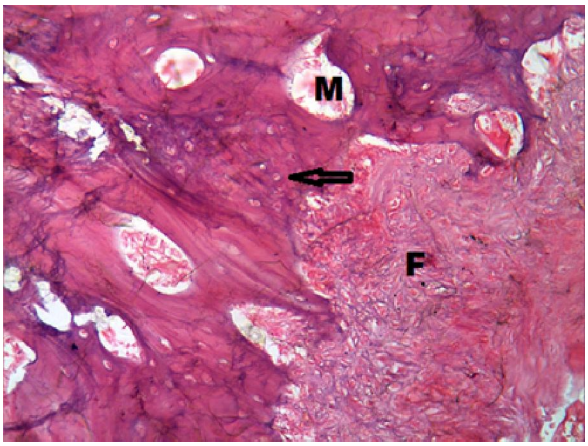

Figure 7. Higher magnification photomicrograph of (IHT) group, 4 weeks post-operatively revealing the presence of parallel dense collagen fibers (F) supplied by tiny blood capillaries. Irregular newly-formed bone trabeculae (arrow), enclosing vascular marrow border the implant site, (H&E x200).

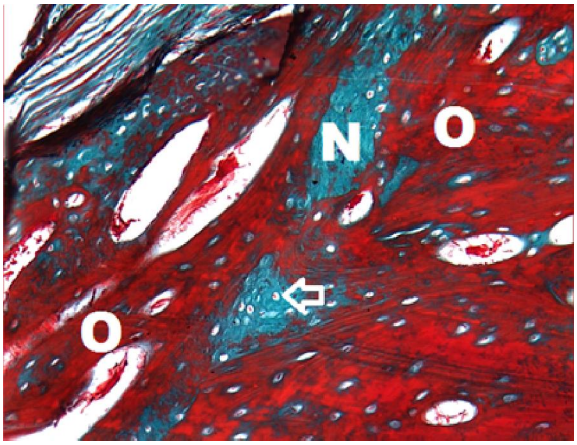

Figure 9. Photomicrograph of (IHT) group at 4 weeks revealing small trabeculae of newly formed bone (N) stained blue- green with Masson's trichrome intermingled with calcified original bone (O) stained red (Masson's trichrome x200).

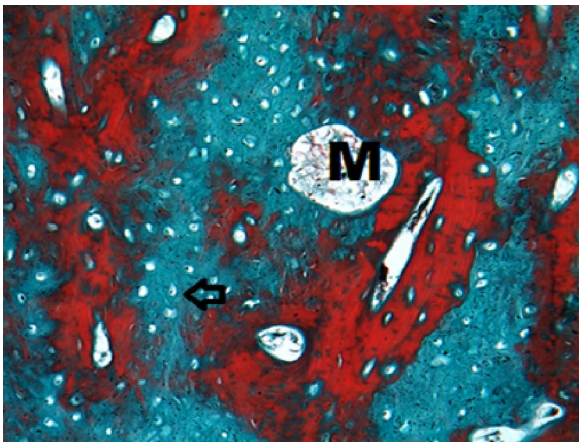

Figure 8. Photomicrograph of (IHT) group at 4 weeks revealing newly formed bone stained blue- green with Masson's trichrome and enclosing viable osteocytes (arrows) intermingled with calcified original bone stained red. Marrow spaces of variable size are also demonstrated (M), (Masson's trichrome x100).

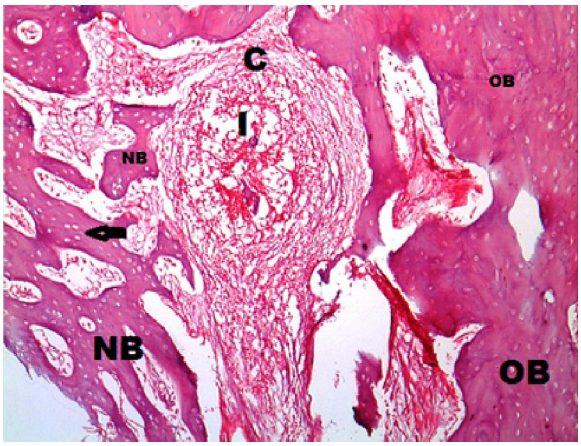

Figure 10. Photomicrograph of TIB group, 8 weeks post-operatively revealing the presence of dilated blood vessels and regular parallel collagen fibers (C) around the implant site (I). Viable osteocytes (arrow) are enclosed in the irregular thin newly formed bone trabeculae (NB) that attempt to fill the interface between the implantation site and the original bone (OB) (H&E x100) .

Figure 11. Higher magnification photomicrograph of TIB group, 8 weeks post-operatively illustrating the dilated blood vessels (B), the extravasated red blood cells and the regular parallel collagen fibers (C) present at the interface between the original bone (OB) and the newly formed bone trabeculae (NB). Numerous osteocytes (arrow) are enclosed in the newly formed trabeculae (H&E x200).

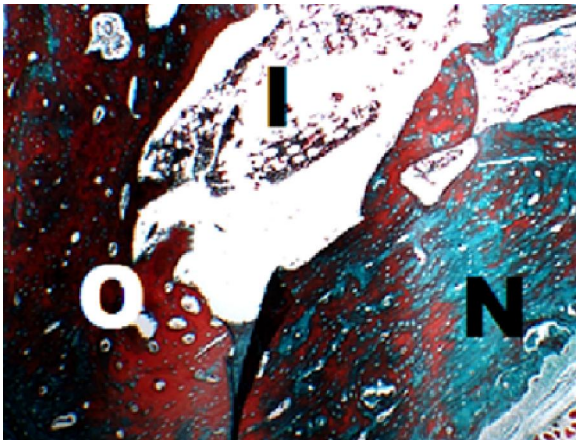

Figure 13. Photomicrograph of (TIB) group at 8 weeks revealing thin trabeculae of newly formed bone (N) stained blue- green with Masson's trichrome bordering the implant site (I). Original bone (O) stained red is also demonstrated (Masson's trichrome x200).

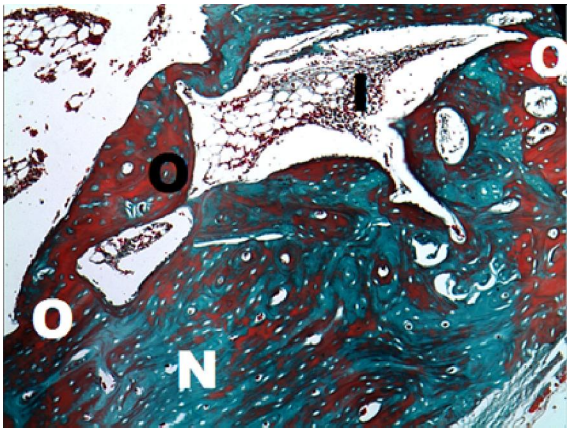

Figure 12. Photomicrograph of (TIB) group at 8 weeks revealing trabeculae of newly formed un-calcified bone (N) stained blue- green with Masson's trichrome bordering the implant site (I). Original bone (O) stained red is also demonstrated (Masson's trichrome x100).

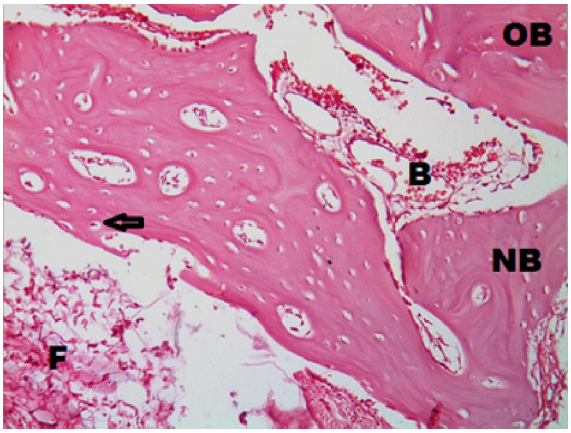

Figure 14. Photomicrograph of (IHT) group, 8 weeks post-operatively revealing the presence of irregular loose connective fibers (F) around the implant site. Irregular newly-formed bone trabeculae enclosing viable osteocytes (arrow) are seen. Dilated blood vessels (B) are demonstrated at the interface between the newly-formed and the original bone (OB), (H&E x100)

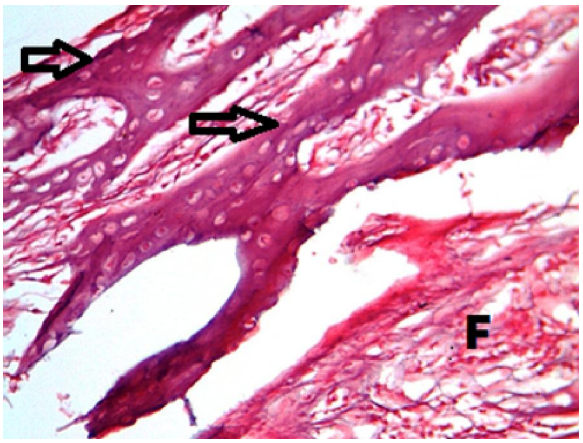

Figure 15. Photomicrograph of (IHT) group, 8 weeks post-operatively illustrating loose fibrous connective tissue (F) at the vicinity of the implant. Thin elongated newly-formed bone trabeculae enclosing viable osteocytes (arrows) and separated by parallel collagen fibers are bordering the implant site (H&E x200)

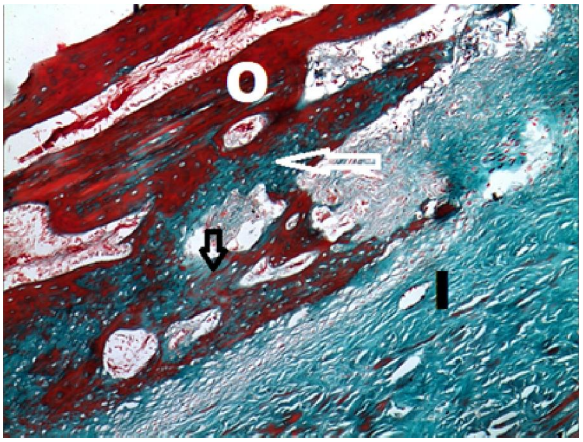

Figure 16. Photomicrograph of (IHT) group at 8 weeks revealing newly formed bone stained blue-green with Masson's trichrome and enclosing viable osteocytes (arrows) bordering the implant site (I) and intermingled with calcified original bone (O) stained red (Masson's trichrome x100).

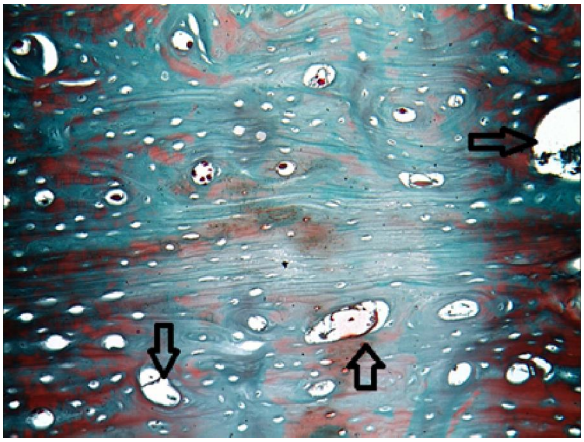

Figure 17. Higher magnification of the previous photomicrograph of (TIB) group at 8 weeks revealing trabeculae of newly formed un-calcified bone stained blue- green with Masson's trichrome . Variable sized marrow spaces (arrows) are also demonstrated (Masson's trichrome x200).

Statistical results

I-Comparison between TIB and IHT

Histomorphometric estimation of the mean area percent filled by bone trabeculae 4 weeks post-operatively was greater in the TIB group (62.31± 13.38) compared to the IHT group (59.38±12.15). Unpaired Student's t test revealed that the difference was not statistically significant (p=0.7263).

On the contrary, eight weeks post-operatively, the area percent of bone trabeculae was greater in the IHT group (90.66±2.87) compared to the TIB group (83.3±3.92). Unpaired Student's t test revealed that the difference was statistically high significant (p=0.0095) (Table 1, Fig. 18)

Table 1. Values of area % filled by bone trabeculae and statistical significance of the different between both groups at each observation period (unpaired Student's t test)

Values	*4 weeks*		*8 weeks*	
	TIB	***IHT***	***TIB***	***IHT***
Mean	62.31	59.38	83.3	90.66
Std Dev	13.38	12.15	3.92	2.87
Std Error	5.982	5.435	1.754	1.281
Max	80.682	79.669	89.534	95.559
Min	42.665	44.944	78.054	87.147
2-s Range	53.502	48.614	15.69	11.462
t value	0.3625		3.3878	
P value	0.7263		0.0095**	

** Statistically high significant

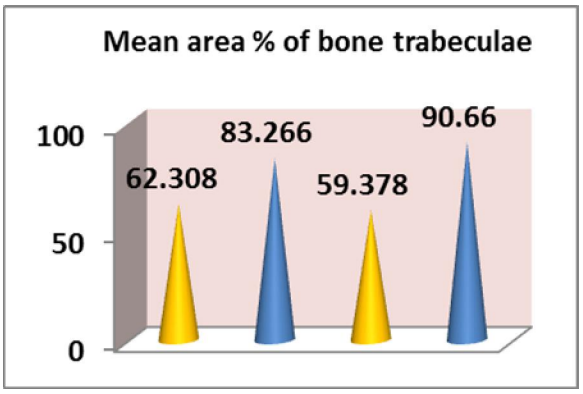

Figure 18. Mean area percent filled by bone trabeculae in both groups

II- Change by time in bone trabeculae in both groups

Both the TIB and IHT groups exhibited an increase in the area percent occupied by bone trabeculae throughout time. Student's t test revealed that the difference in the mean area % throughout the experiment (four and eight weeks post-operatively) was very statistically significant in the TIB group (0.0098**) and IHT groups (0.0005**) indicating an enhancement of bone formation throughout time. The percent increase was greater in the IHT group (52.86%), compared to the TIB group (33.69%), (Table 2, Fig.19-20).

Table (2) Change by time in mean area % of bone trabeculae of each group and statistical significance of the difference (Paired Student's t test)

	TIB		***IHT***	
	4 weeks	8 weeks	4 weeks	8 weeks
Mean	62.31	83.3	59.38	90.66
Std Dev	13.375	3.923	12.153	2.865
% increase	33.69%		52.68%	
t value	3.3673		5.6017	
P value	0.0098**		0.0005**	

** Statistically high significant

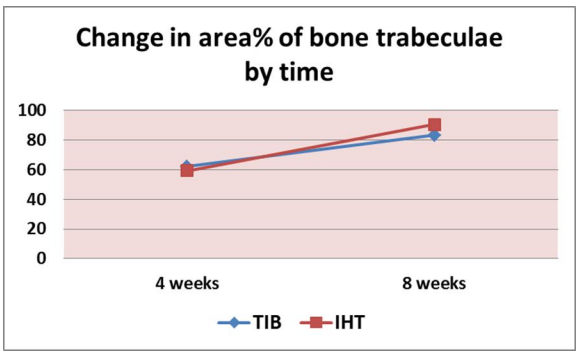

Figure 19. Change by time in area % of bone trabeculae in both groups

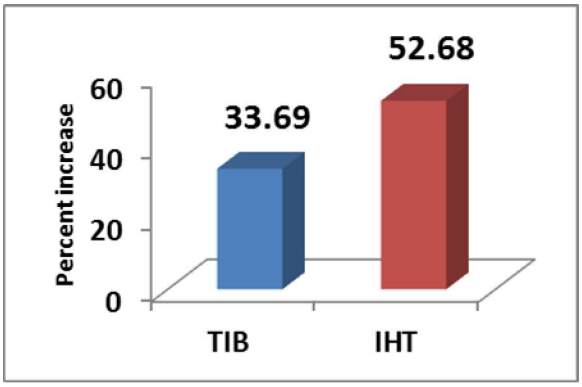

Figure 20. Percent increase in area % filled by bone trabeculae throughout the experiment

4. Discussions

Advances in laser technology open new gates for manufacturing unique products in the dental field. Laser energy is highly focused, precisely penetrative and power controlled. These advantages enabled laser to be used in SLS, which is one of the rapid prototyping manufacturing technique. SLS technique allowed the manufacturer to build the implant fixture totally from titanium alloy powders. In addition, laser was used in another innovative manufacturing technique called computer-controlled laser ablasion technique. This technique is named commercially laser-lok microchannels, which consists of precise three-dimensional microstructures formed by a nanolaser (Aljateeli and Wang, 2013 and Nevins et al., 2008).

The target of the present study was to clarify the efficiency of such new manufacturing techniques in producing suitable implant surface for optimal osseointegration. Accordingly, two implant systems were selected; each of them depends on one of the studied technology. The results of the recent study exhibited statistically significant changes in trabecular bone percent between times within the same group. This finding supports the great success of these surface roughness techniques in implant dentistry. It was also agreed with the several animal studies promoted to follow osseointegration (Novaes et al., 2002, Steigenga et al., 2004, Grew et al., 2008, Gatto et al., 2010, Traini et al., 2008 and Grizona et al., 2002).

This finding confirmed the studiesconducted by Karageorgiou and Kaplan (2005) and Ryan et al., (2006) regarding the optimal implant surface for osseointegration. They added that 0.1 mm seems to be the minimum pore size required for bone ingrowth. There was a consensus that pore sizes range (0.1 and 0.4 mm) are suitable for bone ingrowth. Thus, SLS offers surface topography that could not be created by available manufacturing technique nowadays. It is characterized by

intercommunicating cavities that mimics the bone structure that is difficult to prepare through conventional surface treatment. In addition, researchers recognized that it also resemble bone characteristics on mechanical aspect where the modulus of elasticity of the implant surface is closer to the trabecular bone (Raspanti et al., 2007).

SLS technique performs sufficient porosity required for osseointegration. Researches clarified that porosity is essential to enhance diffusion of nutrients and blood flow, allow cell growth and differentiation, and so permit ideal scaffold environment (Mangano et al., 2006). Additionally, the pore size and interconnectivity promote and control of both bone ingrowth and diffusion of physiological nutrients and gases. They also promote removal of metabolic waste and by-products (Mangano et al., 2006).

The intensive porous microstructure with interconnected porous networks is imperative for 3D uniform cell distribution, survival and migration in vivo. (Jamil et al., 2009 and Myron et al., 2008). These entire outcomes could be the results of the high percentage of trabecular bone contact seen for group II (IHT).

The collar area of group I incorporated the laser-lok technology that also promoted the osseointegration and revealed the results seen for this group. Animal studies compared the osseointegration of the laser microtextured implant collar to the machined collar. The machined collar demonstrated osteoclastic activity with increased saucerization. In contrast, there was an intimate adaptation of the bone to the laser microtextured collar as well as evidence of limited epithelial down-growth and connective tissue attachment to the laser microtextured collar. Twelve-micron grooves showed the best potential for inhibition of fibrous tissue growth relative to bone cell growth. Preciously, 8-µm grooves showed the most effective inhibition of epithelial cell migration across these grooves(Myron et al., 2008, Grew et al., 2007 and Frenkel et al., 2002).Similarly, Boyan and Schwartz (2000), in vitro study, suggested specific surface microstructure spacing and height ranges for optimal cell response. Other dental implant systems have advertised groove-textured surfaces at the coronal aspect of the implant. However, these grooves are substantially larger (200 to 250 µm) and on a cellular level, represent surfaces that do not modulate osteoblastic morphology as effectively as the Laser-Lok (8-12µm) microchannels (Boyan et al., 2000 and Zinger et al., 2005).

These surfaces were found to ideally control orientation of attached cells, prevent cell migration perpendicular to the microgrooves, and substantially inhibit fibroblast growth by inhibiting cell spreading. Specifically, 12-µm grooves showed the best potential for inhibition of fibrous tissue growth relative to bone cell growth, and 8-µm grooves showed the most effective inhibition of cell migration across the grooves, in effect acting as a migration barrier. Thus, organization and orientation is considered the main power of this technology promoting the ideal size for cell adherence, organization and proliferation. Accordingly, the use of nanolaser is compulsory to engrave the highly delicate grooves of laser-lok (Zinger et al., 2005).

Moreover, the results of the trabecular bone percent between groups showed non-significant difference at 4 weeks, changed to be highly significant at 8 weeks. The laser-lok implant surface treatment showed a mean value equal (83.3 %) versus (90.66 %) for the SLS implant at 8 weeks. This finding could be claimed to the great difference in surface areas at which each treatment were applied. It is clear that the SLS implant surface treatment of group II covers approximately all the implant surface merged in bones. On the other hand, laser-lok grooves cover about 3 mm length at the collar while the remaining surface was Resorbable Blast Textured (RBT) body, which is out of the focus of the present study (Soboyejo et al., 2005).It should also be mentioned that neither laser-lok is used to cover an implant surface totally nor limiting the study to the collar area will be logic. Thus, this study deals with the laser-lok product available as a whole not just their outcome on the collar area.

It could be also hypothesized that 4 weeks post-opertively was not enough to investigate the amount of bone formation on the implant surface. In contrast, 8 weeks was sufficient to distinguish significantly this difference. This hypothesis relies on the fact that the delayed loading protocol has the highest clinical rate of success among other loading protocol. It was proved that 4 months in human mandibular arch and 6 months for maxillary arch were recommended time to enable maximum osseointegration
(www.biohorizons.com/taperedinternal.aspx).
Delayed loading protocol gives satisfactory chance for bone formation, organization and integration. (Misch, 2008). Similarly, the 8 weeks period in the selected animal may represent the delayed loading and so maximize the overall results. The present study was designed to entail the tibial bone that constituted mainly compact cortical bone, with a structure comparable to that of human. Hence, the tibia was considered an ideal model for mandibular bone (Chong-Hyun and Dong-Hoo, 1994).

Although the animal studies allow more controlled and organized media for research, further clinical studies should be conducted to augment the

results of this study. Actually, the clinical studies provide several circumstances to be incorporated to enrich the study such as loading and soft tissue evaluation at the collar area.

Advances in the laser technology as a manufacturing tool leads to highly improved implant surface treatment and so enhanced oseointegration. According to the current animal study, the implant surface roughness created by selective laser sintering provided better environment for osseointegration than that produced by engraving microgrooves on titanium surface by nano-laser ablasion.

Acknowledgement
The authors would like to thank the financial support by the Deanship of Scientific Research, Qassim University (grant no.1322).

Corresponding Author:
Dr. Amr Elkarargy
Department of Periodontics, Faculty of Dentistry,
Qassim University, KSA.
E-mail: dr.amr.elkarargy@qudent.org

References

1. Huang HH, Hsu CH, Pan SJ, He JL, Chen CC. Corrosion and cell adhesion behavior of Tin-coated and ion-nitrided titanium for dental application. Appl Surf Sci 2005; 244: 252–6.
2. Faria AC, Beloti MM, Rosa AL. Nitric acid passivation does not affect in vitro biocompatibility of titanium. Int J Oral Maxillofac Implants 2003;18:820–5.
3. Ellingsen JE. Surface configuration of dental implants. Periodontol 2000 1998; 17:36–46.
4. Turner TM, Sumner DR, Urban RM, Rivero DP, Galante JO. A comparative study of porous coatings in a weight-bearing total hip-arthroplasty model. J Bone Joint Surg Am1986;68:1396–409.
5. Reilly DT, Burstein AH, Franklin VH. The elastic modulus of bone. J Biomech 1974; 7:271–5.
6. Rho JY, Roy ME, Tsui TY, Pharr GM. Elastic properties of microstructural components of human bone tissue as measured by nanoindentation. J Biomed Mater Res1999;45:48–54.
7. Barewal RM, Oates TW, Meredith N, Cochran DL.: Resonance frequency measurement of implant stability in vivo on implants with sandblast and acid-etched surface. Int J Oral Maxillofac Implants 2003; 18:641–51.
8. Cooper LF. A role for surface topography in creating and maintaining bone at titanium endosseous implants. J Prosthet Dent 2000; 84:522–34.
9. Esposito M, Coulthard P, Thomsen P, Worthington HV. Interventions for replacing missing teeth: Different types of dental implants. Cochrane Database Syst Rev 2005(1):CD003815
10. Esposito M, Coulthard P, Worthington HV, Jokstad A, Wennerberg A Interventions for replacing missing teeth: different types of dental implants. Cochrane Database Syst Rev 2002(4):CD003815.
11. Esposito M, Murray-Curtis L, Grusovin MG, Coulthard P, Worthington HV. Interventions for replacing missing teeth: different types of dental implants. Cochrane Database Syst Rev 2007(4):CD003815.
12. Esposito M, Worthington HV, Thomsen P, Coulthard P. Interventions for replacing missing teeth: different types of dental implants. Cochrane Database Syst Rev 2003(3):CD003815.
13. Biela SA, Su Y, Spatz JP, Kemkemer R. Different sensitivity of human endothelial cells, smooth muscle cells and fibroblasts to topography in the nano-micro range. Acta Biomater 2009; 5(7):2460-6.
14. Geblinger D, Addadi L, Geiger B. Nano-topography sensing by osteoclasts. J Cell Sci 2010; 123(9):1503-10.
15. Martinez E, Engel E, Planell JA, Samitier J. Effects of artificial microand nano-structured surfaces on cell behaviour. Ann Anat 2009; 191:126-35.
16. Asaoka K, Kuwayama N, Okuno O & Miara I. Mechanical properties and biomechanical compatibility of porous titanium for dental implants. J. Biomed. Mater. Res 1985; 19: 699-713.
17. Yue S, Pilliar R & Weatherly G. The fatigue strength of porous coated Ti 6%A14%V implant alloy. J. Biomed. Mater. Res 1984; 18: 1043-58.
18. Okazaki K, Lee W, Kim D, Kopczyk R. Physical characteristic of Ti-6Al-4V implants fabricated by electrodischarge compaction. J. Biomed. Mater. Res 1991;25: l-13.
19. Lifl M ,Okazaki K. Mechanical properties of a Tip 6Al-4V dental implant produced by electro-discharge compaction. Clin. Mater 1993;14: 13-9.
20. Yang GL, He FM, Yang XF, Wang XX, Zhao SF. Bone responses to titanium implants surface-roughened by sandblasted and double etched treatments in a rabbit model. Oral Surg Oral Med Oral Pathol Oral Radiol Endod 2008; 106:516-24.
21. Deckard C, Beaman JJ. Process and control issues in selective laser sintering. ASME Prod Eng Div (Publication) PED 1988; 33:191–7. (Abstract)
22. Aljateeli M, Wang HL. Implant microdesigns and their impact on osseointegration. Implant Dentistry 2013; 22:127-132.
23. Nevins M, Nevins ML, Camelo M, Boyesen JL, Kim DM.. Human histologic evidence of a connective tissue attachment to a dental implant. Int Journal of Periodont & Resto Dentistry 2008; 28(2), 111-121.

24. Novaes AB Jr, Souza SL, de Oliveria PT, Souza AM. Histomorphometric analysis of the bone-implant contact obtained with 4 different implant surface treatments placed side by side in the dog mandible. Int J Oral and Maxillofac Implants 2002; 17(3):377-383.
25. Steigenga J, Al-Shammari K, Misch C, Nociti Jr. FH, Wang H-L. Effects of implant thread geometry on percentage of osseointegration and resistance to reverse torque in the tibia of rabbits. J Periodontol. 2004; 75(9):1233-1241.
26. Grew JC, Ricci JL, Alexander H. Connective-tissue responses to defined biomaterial surfaces. II. Behavior of rat and mouse fibroblasts cultured on microgrooved substrates. Journal of Biomedical Materials Research Part A. 2008; 85:326-335.
27. Gatto A, Ortolini S Iuliano L. Characterization of S e lec t ive L aser Sintered Implant Alloys: Ti6Al4V And Co-Cr-Mo. In: 20th CIRP Design Conference, Nantes 2010; 20:729-736.
28. Traini C, Mangano R, Sammons F, Mangano A and Macchi A. Direct laser metal sintering as a new approach to fabrication of an isoelastic functionally graded material for manufacture of porous titanium dental implants. Dental materials 2008; 24: 1525–1533.
29. Grizona F, Aguadob E, Hure´c G, Basle´a M, Chappard D. Enhanced bone integration of implants with increased surface roughness: a long term study in the sheep. Journal of Dentistry 2002; 30; 195–203.
30. KarageorgiouV, and Kaplan D. Porosity of 3D biomaterial scaffolds and osteogenesis. Biomaterials 2005; 26: 5474.
31. Ryan G, Pandit, A, and Apatsidis D. Fabrication methods of porous metals for use in orthopaedic applications. Biomaterials 2006; 27: 265.
32. Raspanti M, Mangano C, Macchi A, Mangano F, Piattelli A, Traini T. Morphological investigation of an experimental laser sintered titanium implant. European Journal of Implant Prosthodontics 2007; 1(3):28.
33. Mangano C, Traini T, Piattelli A, Macchi A, Mangano F, Montini S, Mangano A.Producing dental implants by Direct Laser Forming. Italian Oral Surgery 2006; 4:7-12
34. Mangano F, Mangano C, Piattelli A, Iezzi G, Perrotti V. Histologic evaluation of immediately loaded titanium implants. Clinical Oral Implant Research 2006; 17(4):158.
35. Iezzi G, Traini T, Mangano C, Piattelli A. Surface microstructure and fibrine extension on titanium laser sintered specimens. Journal of Clinical Periodontology 2006; 73-80.
36. Jamil Awad Shibli, Carlo Mangano, Susana D' avila, Adriano Piattelli, Gabriele E. Pecora, Francesco Mangano, Tat iana Onuma , Luciana A. Cardoso, Danie l Sanchez Ferrari, Kelly C. Aguiar, Giova nna IezziInfluence of direct laser fabrication implant topography on type IV bone: A histomorphometric study in humans. Journal of Biomedical Materials Research 2009: 607-614.
37. Myron Nevins, Marc L. Nevins,Marcelo Camelo, Janie Lee Boyesen, David M. Kim, Human Histologic Evidence of a Connective Tissue Attachment to a Dental Implant. Int J Periodontics Restorative Dent 2008; 28:111–121.
38. Grew JC, Ricci JL, Alexander H. Connective-tissue responses to defined bio-material surfaces. Part II. Behavior or rat and mouse fibroblasts cultured on microgrooved substrates. J Biomed Mater Res A 2007; 9.
39. Frenkel SR, Simon J, Alexander H, Dennis M, Ricci JL. Osseointegration on metallic implant surfaces: Effects of microgeometry and growth factor treatment. J Biomed Mater Res Appl Biomater 2002;63: 706–713.
40. Boyan BD, Schwartz Z. Modulation of osteogenesis via implant surface design. In: Davies JE (ed). Bone Engineering. Toronto: EM2, 2000:232–239.
41. Zinger O, Zhao G, Schwartz Z, Simpson J, Wieland M, Landolt D, Boyan B. Differential regulation of osteoblasts by substrate microstructural features. Biomaterials 2005; 26:1837–1847.
42. Soboyejo WO, Nemetski B, Allameh S, Marcantonio N, Mercer C, Ricci J. Interactions between MC3T3-El cells and textured Ti6A14V surfaces. J Biomed Mater Res 2002; 62:57–52.
43. WWW.biohorizons.com/taperedinternal.aspx
44. Misch C E. Contemporary Implant Dentistry, 3rd ed. Elsevier Health Sciences; 2008: 623-630.
45. Chong-Hyun M, Dong-Hoo H. A study on shear-bond strength of the interface between bone and titanium plasma-sprayed IMZ implants in rabbits. Int J Oromaxillofac Imp1994; 9(6): 698-707.

10/25/2013